Research Article

Received: 18 April 2016 Revised: 21 May 2016 Accepted article published: 31 May 2016 Published online in Wiley Online Library: 28 June 2016

(wileyonlinelibrary.com) DOI 10.1002/pi.5167

Novel insights on the physicochemical properties of eumelanins and their DMSO derivatives

Luiz GS Albano,[a,†] Eduardo Di Mauro,[b,†] Prajwal Kumar,[c,†] Fabio Cicoira,[c] Carlos FO Graeff[a,d] and Clara Santato[b*]

Abstract

The biopigment eumelanin, ubiquitous in flora and fauna, is made up of chemically heterogeneous macromolecules based on the 5,6-dihydroxyindole and 5,6-dihydroxyindole-2-carboxylic acid building blocks. The exciting possibility of designing eumelanin-based technologies for bioelectronics and sustainable electronics has to be properly assessed by gaining insights on the charge transfer and charge carrier transport in the pigment, preferably in film form, easily amenable to devices. In this work, we report a study on the electrochemical behaviour of films of eumelanin and its derivatives synthesized in dimethyl sulfoxide (DMSO eumelanins) in different aqueous electrolytes, with different chemical compositions and pH. DMSO eumelanins feature an improved solubility in the solvent DMSO, of relevance for processing purposes. The voltammetric currents are higher at relatively low pH (5.5), as expected considering the well-established proton transport properties of the biopigment. Raman spectroscopy and atomic force microscopy performed on eumelanin films were combined with thermogravimetry with the aim of advancing knowledge on the molecular and supramolecular features of synthetic commercially available eumelanin, DMSO eumelanins as well as natural eumelanin (Sepia melanin). The results collected permit unprecedented insights on the physicochemical properties of eumelanin.

Supporting information may be found in the online version of this article.

Keywords: eumelanin; DMSO eumelanin; Sepia melanin; electrochemistry; Raman spectroscopy; thermogravimetry

INTRODUCTION

Eumelanin is a natural pigment found in several biological systems[1,2] where it is responsible for different functions such as pigmentation, photo-protection and thermoregulation.[3,4] In the human body, eumelanin (named hereafter melanin for simplicity) is present in skin, eyes, hair and inner ear. Sepia melanin, obtained from the ink sac of the cephalopod *Sepia officinalis*, has been intensively studied in the last decades because of its similarity to mammalian melanins.[5–8] Furthermore, Sepia melanin has recently been identified as a model to study neuromelanin,[9] another subclass of melanin that accumulates within the dopaminergic neurons.[10] The broad UV – visible absorption, thermal and photo-stability, and humidity-dependent electrical response of melanin, together with its biocompatibility and biodegradability, have fascinated scientists for decades[11–13] and render the pigment an interesting candidate for emerging technologies in the field of bioelectronics and sustainable electronics.[14,15] Melanin forms from the building blocks 5,6-dihydroxyindole (DHI) and 5,6-dihydroxyindole-2-carboxylic acid (DHICA) (Scheme 1) and their redox forms, hydroquinone, semiquinone and quinone.[16] From four to eight building blocks form planar covalently bonded oligomers (protomolecules) that stack via $\pi-\pi$ interactions to form onion-like nanostructures.[17]

Despite melanin's attractive physicochemical properties, the demonstration of melanin-based technologies represents a serious challenge since melanin is chemically heterogeneous and exhibits low solubility in common solvents.[1–3] Several synthetic routes *in vitro* have been explored to overcome these obstacles.[18–21] Recently, a method for *in situ* controlled deposition of melanin nanoparticles from the enzymatic reaction of L-3-(3,4-dihydroxyphenyl)-alanine (L-DOPA) with tyrosinase resulting in films with controlled growth and thickness has been reported.[22] The oxidation of L-DOPA with benzoyl peroxide in dimethyl sulfoxide (DMSO) leads to the synthesis of DMSO

* *Correspondence to: C Santato, Département de Génie physique, Polytechnique Montréal, C.P. 6079, Succ. Centre-ville, Montréal, Québec, Canada H3C 3A7. E-mail: clara.santato@polymtl.ca*

† *These authors contributed equally to the work.*

a *UNESP – Univ Estadual Paulista, POSMAT – Programa de Pós-Graduação em Ciência e Tecnologia de Materiais, Bauru, SP, Brazil*

b *Département de Génie physique, Polytechnique Montréal, CP 6079, Succ. Centre-ville, Montréal, Québec, Canada H3C 3A7*

c *Département de Génie chimique, Polytechnique Montréal, CP 6079, Succ. Centre-ville, Montréal, Québec, Canada H3C 3A7*

d *DF-FC, UNESP – Univ Estadual Paulista, Av. Eng. Luiz Edmundo Carrijo Coube 14-01, 17033-360, Bauru, SP, Brazil*

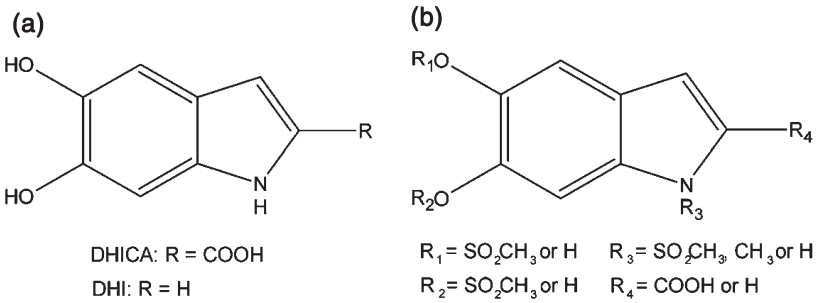

Scheme 1. (a) Building blocks of eumelanin (DHI and DHICA) and (b) DMSO melanins.

melanin (Scheme 1), with good solubility in DMSO, functional for the production of high quality films.[23–29] Increasing the temperature during the synthesis of the DMSO melanin significantly increases the reaction rate and induces the decarboxylation of DHICA, thus increasing the number of positions available in the molecule for polymerization.[26]

Hydrated films of melanin and DMSO melanin included between gold electrodes[28] have been studied in the presence of an electrical bias. The fact that the formation of electrically conductive dendrimers was observed only for non-derivatized melanin was attributed, at least in part, to the limited chelating properties of the building blocks of DMSO melanin. The presence of sulfonated groups in DMSO melanin prevents an effective chelating action at the gold electrodes.

Despite the possibility offered by DMSO melanin to produce homogeneous and smooth films, of relevance for technological applications such as melanin-based cathodes[30] and anodes,[31] the electrochemical properties of DMSO melanin, possibly related to the electrochemical properties of non-derivatized melanin, are largely undiscovered.

In this work, a comparative study was performed to gain insight on the electrochemical activity of DMSO melanin with respect to the commercially available, non-derivatized, Sigma melanin, prepared by oxidation of tyrosine with hydrogen peroxide. Cyclic voltammetry measurements were performed using melanin-based working electrodes in aqueous electrolytes. Raman spectroscopy and AFM, complemented by TGA, contributed to advance knowledge about the physicochemical properties of melanin and melanin derivatives for application in biocompatible coatings, bioelectronic interfaces and human and environmentally friendly electrochemical energy storage solutions.

EXPERIMENTAL

Materials

Sigma melanin (powder), Sepia melanin (powder), L-DOPA, benzoyl peroxide, acetonitrile, acetic acid and phosphate buffered saline (PBS) tablets were purchased from Sigma-Aldrich (Ontario, Canada). DMSO and ammonium acetate (NH_4CH_3COO) were purchased from Caledon Laboratories (Ontario, Canada). Acetate buffer (from acetic acid and KOH) pH 5 was purchased from ACROS Organics (New Jersey, NJ, USA). Porous carbon paper (2050 series) was purchased from Spectracarb (Shelton, CT, USA) with 10 mils and 0.2 mm thickness.

Synthesis and processing of melanins and fabrication of films

DMSO melanin synthesized at room temperature (RT) and DMSO melanin synthesized at 100 °C were obtained as already reported in the literature.[25,26]

Melanin films were spin-coated on previously cleaned glass substrates (2.5 cm × 2.5 cm) from DMSO suspensions, 30 mg mL^{-1} (1 min at 1000 rpm, then 30 s at 4000 rpm).

Raman spectroscopy

Raman measurements were carried out using a Renishaw Invia reflex confocal Raman microscope with a CCD detector. Raman spectra were collected at room temperature with 10% of maximum laser power, 30 s exposure time and five accumulations in static mode. A 1800 lines mm^{-1} grating was used in conjunction with 25 mW, 488 nm and 514 nm laser lines, focused on the samples using a 50× objective lens. Five samples of each type of melanin were measured and different points (at least three) were considered for each sample. To properly identify the functional groups, Raman spectra were fitted through deconvolution with Gaussian functions using Origin Pro 8.5.1. Before fitting, a baseline was performed for each spectrum in order to remove luminescence effects.

Thermogravimetry

TGA was performed using a TA Instruments TGA 2950 thermogravimetric analyser. Tests on the powders conditioned for 24 h were performed in the range 25–500 °C (25–700 °C only for Sepia melanin at 70% relative humidity) under a nitrogen atmosphere (90 cm^3 min^{-1}) at a heating rate of 10 °C min^{-1}. Tests on powders hydrated for less than 24 h were performed in the range 25–1000 °C under an argon atmosphere (90 cm^3 min^{-1}) at a heating rate of 10 °C min^{-1}. Powders were conditioned in a Cole-Parmer mini humidify/dehumidify chamber (03323–14), with an automatic humidity controller and an ultrasonic humidification system. It should be noted that, between the conditioning at a certain relative humidity level and the beginning of each TGA, the powders were at ambient relative humidity for a few seconds during the loading in the TGA furnace. The number of samples investigated is specified in the Supporting information.

AFM and thickness measurements

AFM measurements, performed on films fabricated as for the Raman investigations, were taken using an atomic force microscope Dimension 3100 (Digital Instruments) with Si probes (tip radius <10 nm, spring constant 42 N m^{-1}) in tapping mode. AFM images were analysed with Bruker Nanoscope Analysis. Film thickness was measured using a Dektak 150 profilometer (after scratching the film with a blade). Four films for each type of melanin were measured by AFM and profilometry.

Electrolytes

NH_4CH_3COO pH 5.5 (1 M and 7.5 M) was prepared in deionized water (a few drops of acetic acid were added to bring the pH of the solution to 5.5). PBS electrolyte at pH 7.4 was obtained by dissolving one tablet (1.8–2 g tablet^{-1}) in 200 mL of deionized water, which yields 0.01 M phosphate, 0.0027 M potassium chloride and 0.137 M sodium chloride, pH 7.4, at 25 °C.

Electrochemistry

Cyclic voltammetry was performed using a software-controlled (EC-Lab V10.39) Multi Potentiostat VSP 300 from Biologic Science Instruments. A carbon paper strip acted as the counter electrode and aqueous silver chloride (0.197 V *versus* SHE) as the reference electrode. The electrochemical cell was purged with N_2 to limit the O_2 presence during the measurements.

Fabrication of melanin electrodes on carbon paper (Mel/CP electrodes)

A melanin suspension was prepared by mixing 3 mg mL^{-1} of melanin in DMSO in a planetary mixer (Thinky ARM-310) at 2000 rpm for 30 min. 10 µL of suspension drop-cast onto carbon paper (geometric area of 0.25 cm^2), dried at 55 °C under vacuum (*ca* 40 mbar) for 2 h to facilitate DMSO removal, acted as the working electrode. Five working electrodes per type of melanin were measured.

RESULTS AND DISCUSSION

Raman spectroscopy

Raman spectroscopy was used to gain insight on the molecular structure of the melanins investigated in this work. Both, films fabricated by spin-coating and powders were considered. Raman spectra indicate that films and powders do not differ significantly in their molecular structure, thus suggesting, as expected, that the processing steps do not affect the molecular structure of melanin. A considerable number of vibrational modes contribute to the Raman spectra (Figs 1 and S1, Tables S1 and S2). Bands G (at *ca* 1590–1605 cm^{-1}) and D (at *ca* 1350–1380 cm^{-1}) are the dominant modes and are attributable to disordered graphitic carbon.[32–34]

Contributions of the quinone C=O stretching are observable at about 1690 cm^{-1} whereas contributions from C=N ring stretching (from semiquinone structure) and N–H bending vibrational modes are observable at 1510 cm^{-1} [33] for Sigma melanin and 1535 cm^{-1} for DMSO melanins. The band at 1771 cm^{-1} for Sigma melanin can be assigned to C=O stretching in carboxylic acid.[33–35] The absence of such band for DMSO melanins can be related to the presence of the sulfonated groups.[25,26] The mode at

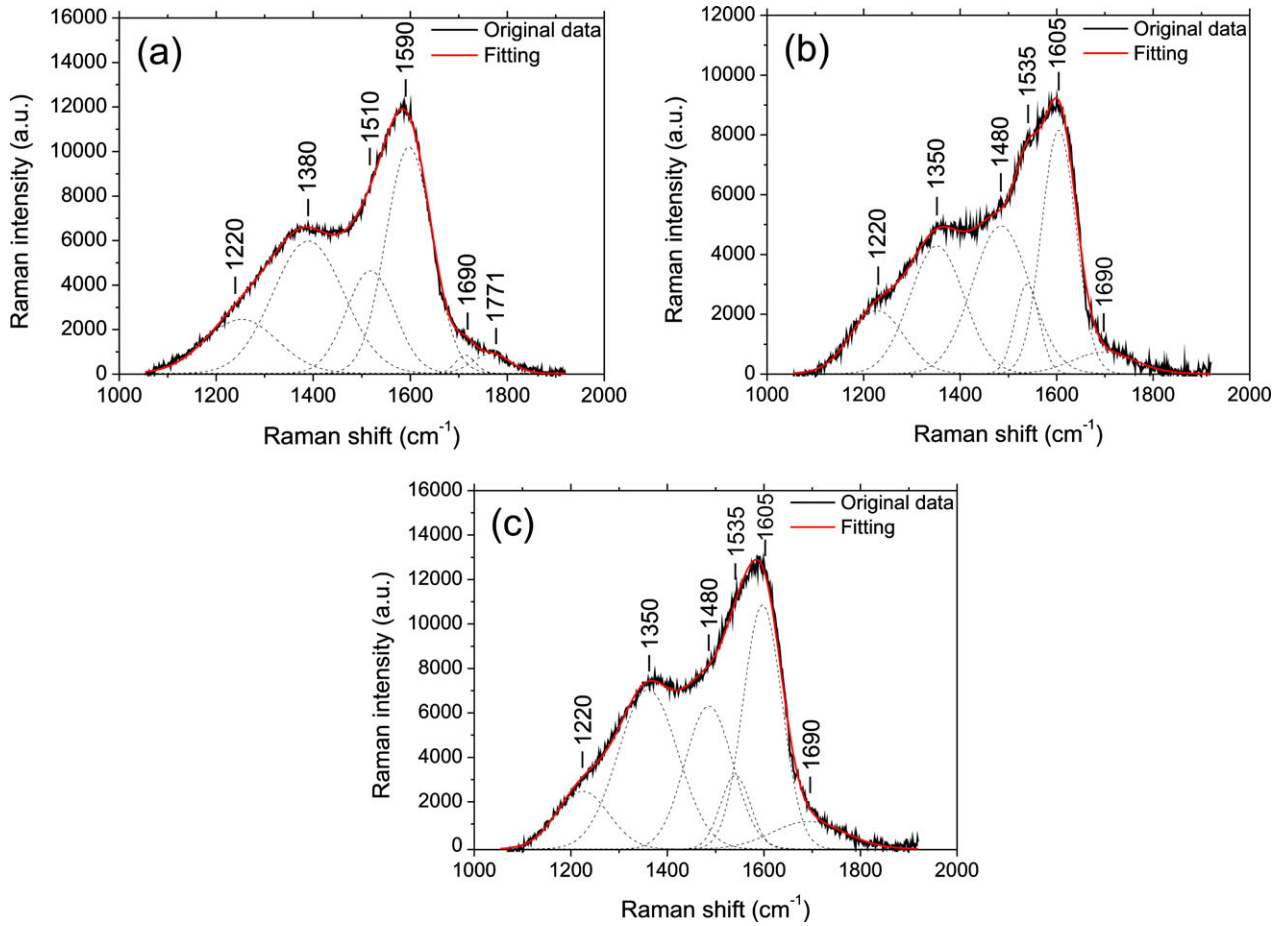

Figure 1. Raman spectra for the melanin films deposited by spin-coating on glass substrates investigated in this work: (a) Sigma melanin; (b) DMSO melanin RT; (c) DMSO melanin 100 °C. Experimental Raman spectra (black, continuous line), spectra resulting from a deconvolution of the experimental bands by means of Gaussian bands (black dashed lines) and the sum of the Gaussian bands (red continuous line) are shown. The location of the bands G and D were fixed during the fitting procedure: 1590–1380 cm^{-1} for Sigma melanin, 1605–1350 cm^{-1} for DMSO melanins. The quality of the fitting is remarkable: (a) chi-squared is 0.99921, (b) chi-squared is 0.99638 and (c) chi-squared is 0.99983.

1220 cm^{-1} is attributable to C – OH phenolic stretching and C – O stretching of carboxylic acid.[34,35]

Thermogravimetric analysis

TGA was carried out in order to gain insights into the water content of the pigment and its molecular and supramolecular structure, both dramatically affecting the functional properties of the pigment.

Each minimum of the thermogravimetric derivative (DTG) corresponds to the completion of a thermogravimetric phenomenon, while the abscissa of each maximum of the DTG represents the temperature at which the thermogravimetric phenomenon takes place at its fastest rate; examples of thermogravimetric phenomena taking place are water loss and the decomposition of the protomolecules as well as of the nanostructures that make up the biomaterial.

The TGA of Sigma melanin reveals three main phenomena associated with five extrema of the DTG (Fig. 2(a), Tables S3 and S4). The weight loss until the first minimum of the DTG, occurring at 130 ± 4 °C, can be ascribed to the loss of weakly bound water.[29,36–39] Other low molecular weight molecules, such as ammonia, may be removed in this temperature range.[40] The second phenomenon, taking place between 130 ± 4 °C and 731 ± 46 °C, may be ascribed to the decarboxylation of the DHICA units,[40] reported in the literature[41] in a range in good agreement with the position of extremum 3.1, 220 ± 15 °C, as well as to the rupture of the covalent bonds formed during the melanin polymerization, implying the evolution of CO_2.[42] Degradation of uncycled moieties cannot be excluded considering the fact that the decomposition of tyrosine has been reported between 250–400 °C.[43] The last phenomenon, starting at 731 ± 46 °C and not completed at 1000 °C, may be tentatively associated with the rupture of covalent bonds, the decomposition of indole and pyrrole rings, possibly accompanied by the evolution of CO_2 and NH_3.[40]

The typical TGA for DMSO melanin RT comprises five decomposition steps whereas DMSO melanin 100 °C only comprises three (Fig. 3, Tables S5–S8), with the first two decomposition steps being the same for both.

Surprisingly, and differently from Sigma melanin, no minimum related to water loss can be detected. The weight loss at 150 °C is 1.8% ± 0.2% for DMSO melanin RT and 1.0% ± 0.1% for DMSO

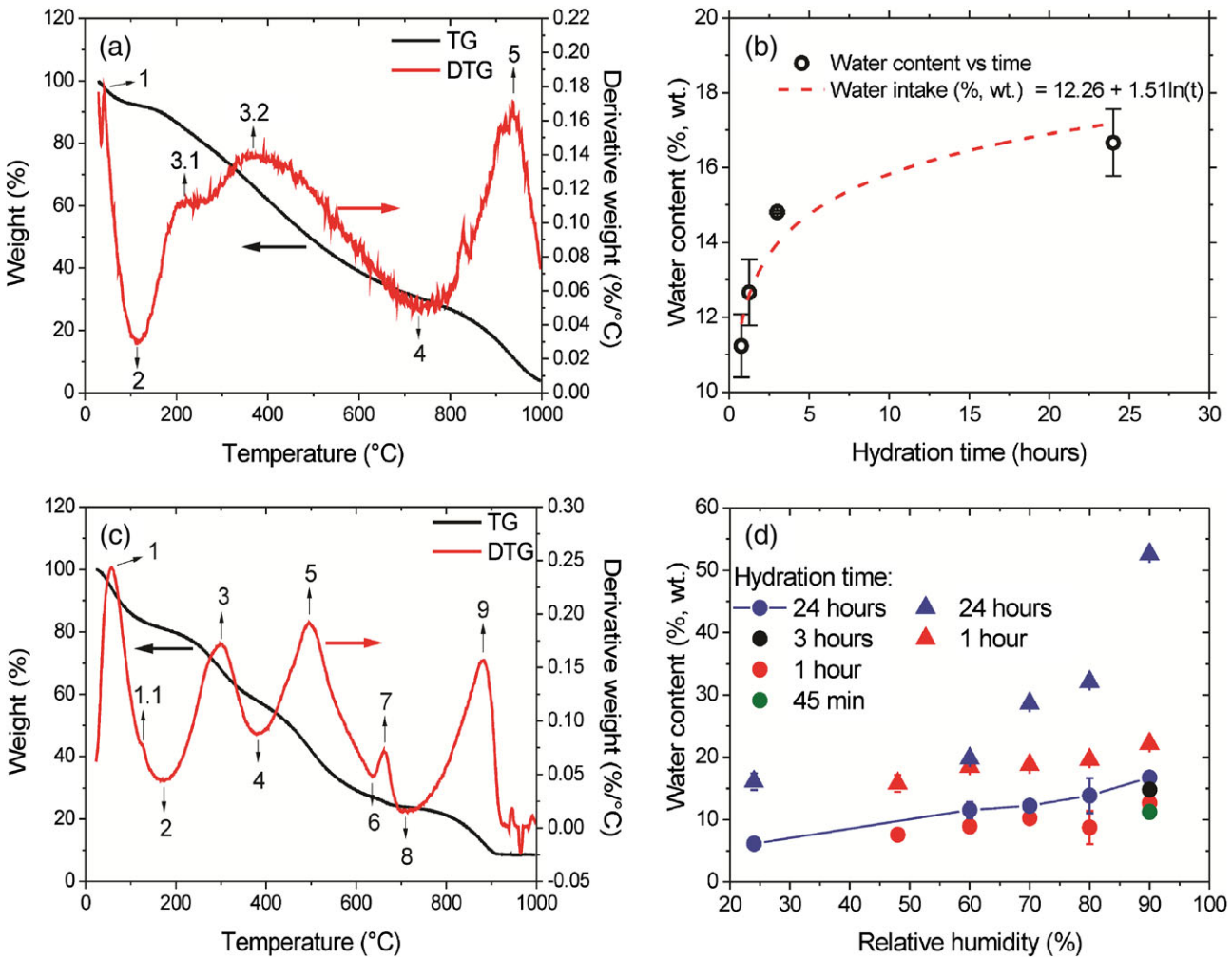

Figure 2. Thermogravimetry and water content analyses. (a) Thermogravimetry and DTG of Sigma melanin powder hydrated for 1 h at 48% relative humidity; the numbers refer to the extrema of the DTG (Table S4). (b) Water intake *versus* hydration time of Sigma melanin. The dashed line refers to the logarithmic law that describes the absorption trend. (c) TGA and DTG of Sepia melanin powder hydrated for 1 h at 70% relative humidity; extrema in the DTG as in Table S10. (d) Water content *versus* relative humidity (circles correspond to Sigma melanin and triangles to Sepia melanin). The line is a guide for the eye for the data for Sigma melanin, 24 h hydration, taken from a previous work.[16]

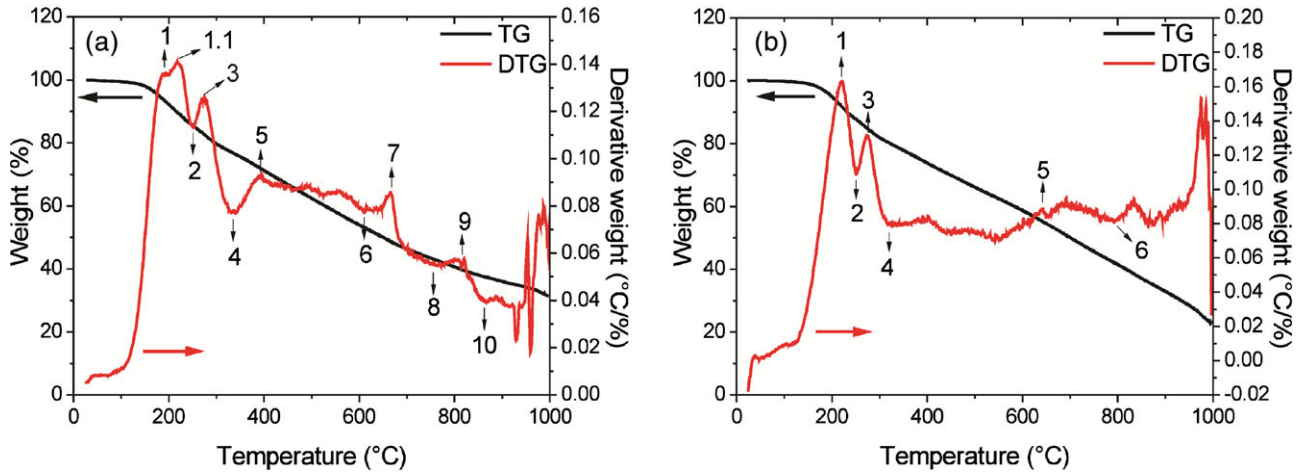

Figure 3. Thermogravimetric analysis: (a) DMSO melanin RT, powder; (b) DMSO melanin 100 °C, powder. The numbers refer to the extrema of the DTG (Tables S6 and S8).

melanin 100 °C, in good agreement with previous work.[29,44] The negligible amount of water can be ascribed to the non-aqueous medium employed during the synthesis and to the subsequent storage in an N_2 glovebox. In both cases, the minimum of the DTG located at approximately 350 °C (extremum 4, Tables S6 and S8) can be associated with the beginning of the desulfonation, as reported in the literature.[45,46] The weight left at 1000 °C (35% ± 5% for DMSO melanin RT and 30% ± 10% for DMSO melanin 100 °C) is most probably composed of graphitic-like sheets.[29]

In order to obtain a deeper insight on the molecular and supramolecular structure of melanins, we extended our thermogravimetric survey to natural melanin (Sepia melanin, extracted from the ink sac of a cuttlefish). The thermal degradation for Sepia melanin (Fig. 2(c), Tables S9 and S10) shows similarities with Sigma melanin. Nonetheless, a second maximum in the DTG is observable at 124 ± 5 °C, which partially overlaps with the first and shifts the completion of the water loss at higher temperatures. The temperature at which the first minimum of the derivative (water loss) takes place is slightly higher than for Sigma melanin, 171 ± 5 °C, in good agreement with the literature.[44] The second maximum could tentatively be ascribed to the loss of strongly bound water; however, in the literature it has been reported at higher temperatures.[47,48] The second decomposition step can be tentatively ascribed to the decarboxylation of DHICA building blocks[41] as well as to the rupture of the supramolecular structure and substructure of natural melanin and to the non-covalent bonds between layers in oligomer planes.[47] The further three steps are associated with breaking of the bonds between the indole units and to the opening of pyrrole and indole rings.[47] The presence of a higher number of decomposition steps for Sepia than for Sigma melanin can be explained considering that the supramolecular structure of Sepia melanin is more complex than Sigma melanin, conferring the ability to 'store' both weakly and hardly bound water[49] as well as implying multiple degradation steps during its heating.

Different relative humidity levels and hydration times were studied for Sigma and Sepia melanin (Fig. 2(d)). Concerning the hydration kinetics for Sigma melanin, after 24 h of conditioning most of the water present (>75%) was actually absorbed during the first hour (Fig. 2(b)). The higher the relative humidity level is, the more Sepia melanin absorbs water (as much as half of the weight of the pigment is ascribable to water for a conditioning of 24 h at 90% relative humidity, in good agreement with what was reported in the literature[4]). Concerning the hydration kinetics, the higher the relative humidity level is, the smaller is the percentage of water absorbed in the first hour with respect to the amount after 24 h. This may tentatively be explained considering that for longer hydration times water is able to 'soak' into the most remote crevices contributing to the hardly bound water fraction. Analysing Fig. 2(d) it may be inferred that Sepia melanin is more hygroscopic than Sigma, as opposed to dopa-melanin.[49] It is worth noting that the conditioning at different relative humidity levels does not influence either the position of the extrema or the weight losses related to different decomposition phenomena (Figs S2, S3, S4 and S5), except for the first one (water loss) already discussed.

Atomic force microscopy

The morphologies of the spin-coated films prepared from Sigma melanin, DMSO melanin RT and DMSO melanin 100 °C were studied by AFM. AFM permits light to be shed on the continuity of the films, the degree of coverage of the substrate and the smoothness of the surface, key parameters to assess the applicability of films in device architectures. Films obtained from Sigma melanin showed the highest root mean square roughness (Rq), i.e. 0.40 ± 0.17 nm, followed by DMSO melanin 100 °C (0.29 ± 0.11 nm) and DMSO melanin RT (0.14 ± 0.06 nm; Fig. 4, Table S11). The corresponding thicknesses measured by profilometry were found to be about 57 ± 4, 42 ± 6 and 31 ± 3 nm (Fig. S6, Table S11). Thicker films, obtained after three sequential spin-coating runs from the same three types of melanin, were found to be about 155 ± 9, 131 ± 8 and 114 ± 7 nm thick. Their Rq showed the same tendency as for their thin counterparts, i.e. 0.70 ± 0.16, 0.58 ± 0.19 and 0.42 ± 0.09 nm (Fig. 4, Table S12).

The low roughness of the films obtained from DMSO melanins is probably due to their good solubility in DMSO.[25] Moreover, the relatively high temperature required to prepare DMSO melanin 100 °C, promoting a relative increase in DHI concentration and leaving, at the same time, an increased number of positions available for polymerization,[26] is likely to be the cause of an increased roughness and thickness for DMSO melanin 100 °C with respect to DMSO melanin RT. A considerable number of agglomerates are observed for DMSO melanin 100 °C compared with DMSO melanin RT, probably related to a higher polymerization degree.

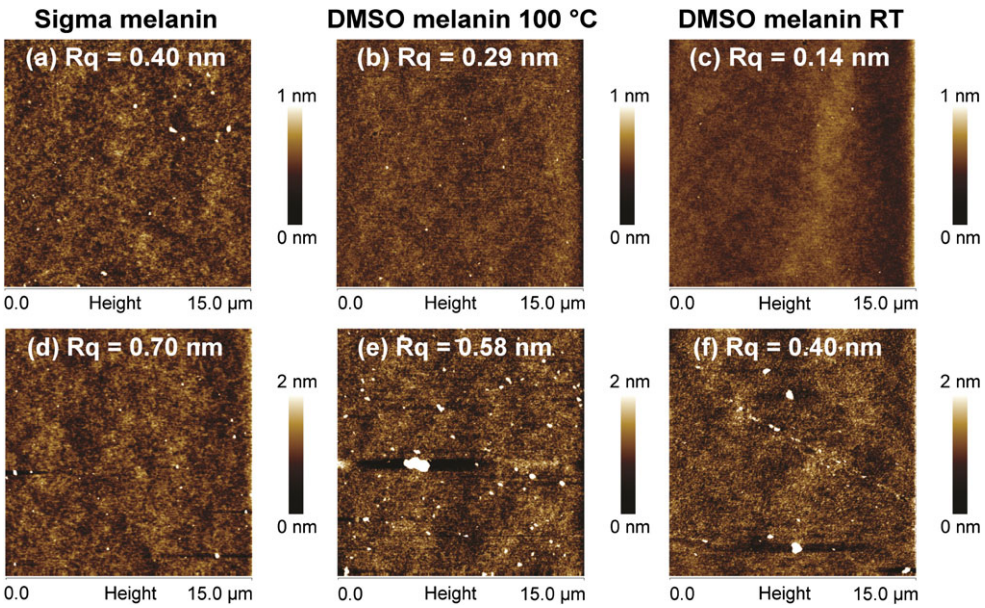

Figure 4. 15 µm × 15 µm AFM topography images of spin-coated melanin films: (a) – (c) melanin thin films with one spin-coating run; (d) – (e) melanin thick films with three sequential spin-coating runs.

Cyclic voltammetry

To gain insight into the electron transfer properties of Sigma melanin, DMSO melanin RT and DMSO melanin 100 °C, their electrochemical behaviour was investigated by cyclic voltammetry.[50,51] The working electrode was constituted by melanin drop-cast from DMSO suspensions onto carbon paper, with 120 µg cm^{-2} melanin loading. Electrolytes with different chemical compositions and with different pH were employed to gain insight on the effect of the electrolyte on the electrochemical behaviour of melanin: 7.5 M NH_4CH_3COO pH 5.5 and PBS pH 7.4 (Figs 5, S7 and S8).

As a general observation, the voltammetric currents are higher at relatively low pH, as expected considering the well-established proton transport properties of melanin.[16]

Independently of the type of melanin and electrolyte, during the first two to three voltammetric cycles a broad, irreversible anodic response is observed,[16] between 0.25 and 0.9 V *versus* Ag/AgCl for 7.5 M NH_4CH_3COO pH 5.5 and between 0.15 and 0.9 V *versus* Ag/AgCl for PBS pH 7.4. Such anodic response is attributable, at least in part, to the formation of oxidized species at the positive electrode, eventually coupling to lead an increased intermolecular reticulation.[5,16,52] For Sigma melanin, the broad signal includes, during the first cycle, a shoulder located at about 0.4 V *versus* Ag/AgCl.

The cyclic voltammograms of DMSO melanin RT and DMSO melanin 100 °C show, for the first three to four cycles, a shoulder located at about 0.4 V *versus* Ag/AgCl in 7.5 mol L^{-1} NH_4CH_3COO at pH 5.5 and at 0.35 V *versus* Ag/AgCl in PBS pH 7.4. For these two types of melanin, a cathodic peak at about 0.25 V *versus* Ag/AgCl is observable, during the first three to four cycles, in 7.5 mol L^{-1} NH_4CH_3COO at pH 5.5. The cathodic peak shifts to 0.1 V *versus* Ag/AgCl in PBS pH 7.4. The difference in the cyclic voltammograms of DMSO melanins with respect to Sigma is probably due to the sulfonate termination. The contribution due to the possible oxidation of species susceptible to polymerization at the positive electrode, already discussed for Sigma melanin, has to be contemplated even for the DMSO melanins.

Interestingly, for the three melanins investigated, a (pseudo) capacitive behaviour is observable after the third cycle, where voltammograms exhibit a quasi box-shape.

To better understand the effect of the concentration, composition and pH of the electrolyte on the cyclic voltammograms in acetate-based medium, i.e. the medium where the highest voltammetric currents were recorded, additional electrochemical studies were performed, focusing on Sigma melanin (Figs S9 and S10). The concentration does not play a primary role in the voltammetry whereas the acetate buffer at pH 5 shows an anodic peak at around 0.7 V *versus* Ag/AgCl persistent even under prolonged biasing. This peak may be attributed to the oxidation of the building blocks to the quinone form with consequent favourable interaction with K^+ ions from the buffer; the species resulting from such an interaction might dissolve during the cathodic scan, where the quinone form is reduced to hydroquinone.

CONCLUSIONS

With the aim of designing technologies based on the biocompatible, biodegradable, abundant at low cost biopigment melanin, we performed a systematic comparison between commercially available Sigma melanin and melanin derivatives synthesized in DMSO (DMSO melanin) characterized by an improved solubility in common solvents. After a Raman spectroscopy investigation of the different types of melanin, we characterized by scanning probe microscopy films based thereon for their continuity and smoothness. We confirmed the enhanced processability of films based on DMSO melanin. TGA showed that a negligible amount of water is included in DMSO melanin. An extension of the TGA to natural Sepia melanin showed a higher number of decomposition steps for Sepia than for Sigma melanin, attributable, among other factors, to the ability of the former to store both weakly and hardly bound water. The results of the thermogravimetric studies are of primary importance for the development of melanin-based technologies exploiting the proton transport properties of the pigment. Spectroscopic,

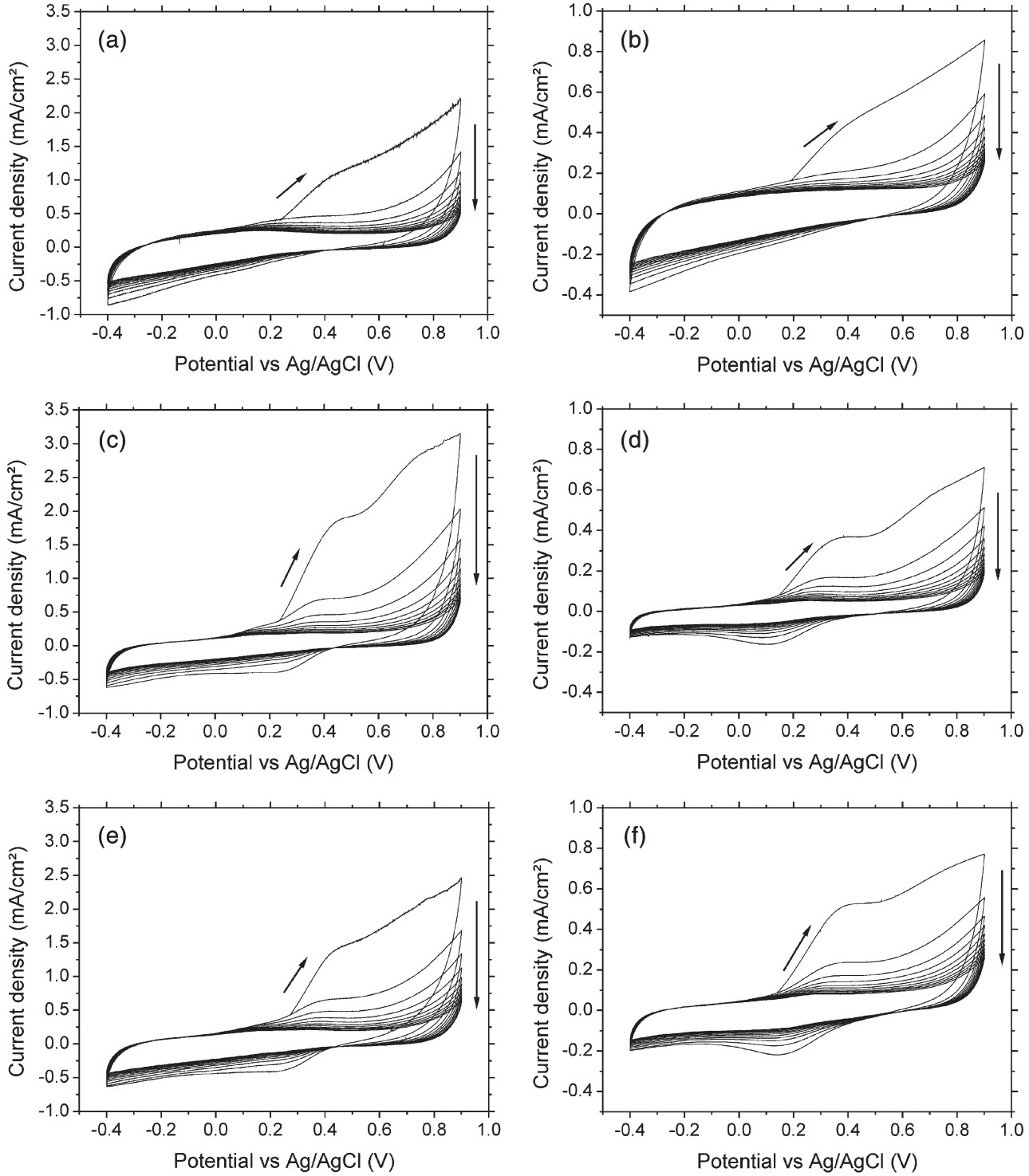

Figure 5. Cyclic voltammograms (total 10 cycles) of different types of melanins in 7.5 mol L^{-1} NH_4CH_3COO pH 5.5 and PBS pH 7.4 electrolytes; 120 μg cm^{-2} of melanin on carbon paper is the loading in the working electrode. (a), (b) Sigma melanin; (c), (d) DMSO melanin RT; (e), (f) DMSO melanin 100 °C. Voltammograms (a), (c) and (e) are in 7.5 mol L^{-1} NH_4CH_3COO pH 5.5, whereas (b), (d) and (f) are in PBS pH 7.4. Carbon paper strips were used also as counter electrode; scan rate 50 mV s^{-1}; geometric area of the working electrode 0.25 cm^2.

topographical and thermogravimetric studies were the underpinning for the exploration of the electrochemical properties of the films. Cyclic voltammetry shows that currents are higher in electrolytes with relatively low pH, in agreement with the well-established proton transport properties of melanin. The originality of our contribution consists in advancing the knowledge about molecular structure, film morphology and functional properties in melanin films to try to predict the performance of devices based thereon. Our findings are indeed functional for an improved design of melanin-based technologies for applications such as neural interfaces and electrochemical energy storage.

ACKNOWLEDGEMENTS

We gratefully acknowledge FAPESP (2014/25332-9), CEPID (2013/07296-2), MDEIE (CS), FQRNT (CS and FC) and NSERC (Discovery grants CS and FC) for financial support. We thank Dr E. Samir and P. Moraille for assistance in Raman spectroscopy and AFM, and Y. Drolet for technical support. We also thank Dr E. S. Bronze-Uhle for fruitful discussions and J. V. Paulin for assistance during the synthesis of DMSO melanins.

SUPPORTING INFORMATION

Supporting information may be found in the online version of this article.

REFERENCES

1 Prota G, *Melanins and Melanogenesis*. Academic Press, San Diego, CA, pp. 1–13 (1992).
2 Ito S, *Pigment Cell Res* **16**:230–236 (2003).
3 McGinness J, Corry P and Proctor P, *Science* **183**:853–855 (1974).
4 White LP, *Nature* **182**:1427–1428 (1958).
5 Pezzella A, d'Ischia M, Napolitano A, Palumbo A and Prota G, *Tetrahedron* **53**:8281–8286 (1997).
6 Centeno SA and Shamir J, *J Mol Struct* **873**:149–159 (2008).
7 Larsson B and Tjälve H, *Biochem Pharmacol* **28**:1181–1187 (1979).
8 Bush WD and Simon JD, *Pigment Cell Res* **20**:134–139 (2007).
9 Schroeder RL, Double KL and Gerber JP, *J Chem Neuroanat* **64**:20–32 (2015).
10 d'Ischia M, Napolitano A, Ball V, Chen C and Buehler MJ, *Acc Chem Res* **47**:3541–3550 (2014).
11 Rosenberg B and Postow E, Ann N *Y Acad Sci* **158**:161–190 (1969).
12 Powell MR and Rosenberg B, *J Bioenerg* **1**:493–509 (1970).
13 Potts AM and Pin CA, *Agressologie* **9**:225–230 (1968).
14 Meredith P, Powell BJ, Riesz J, Nighswander-Rempel SP, Pederson MR and Moore EG, *Soft Matter* **2**:37–44 (2006).
15 Meredith P and Sarna T, *Pigment Cell Res* **19**:572–594 (2006).
16 Wünsche J, Deng Y, Kumar P, Di Mauro E, Josberger E, Sayago J *et al.*, *Chem Mater* **27**:436–442 (2015).
17 Subianto S, Will G and Meredith P, *Polymer* **46**:11505–11509 (2005).
18 Lawrie KJ, Meredith P and McGeary RP, *Photochem Photobiol* **84**:632–638 (2008).
19 Pezzella A, Iadonisi A, Valerio S, Panzella L, Napolitano A, Adinolfi M *et al.*, *J Am Chem Soc* **131**:15270–15275 (2009).
20 Ju K-Y, Lee Y, Lee S, Park SB and Lee J-K, *Biomacromolecules* **12**:625–632 (2011).
21 Cicco SR, Ambrico M, Ambrico PF, Talamo MM, Cardone A, Ligonzo T *et al.*, *J Mater Chem C* **3**:2810–2816 (2015).
22 Strube OI, Büngeler A and Bremser W, *Biomacromolecules* **16**:1608–1613 (2015).
23 Da Silva MIN, Dezidério SN, Gonzalez JC, Graeff CFO and Cotta MA, *J Appl Phys* **96**:5803–5807 (2004).
24 Lorite GS, Coluci VR, Da Silva MIN, Dezideriо SN, Graeff CFO, Galvao DS *et al.*, *J Appl Phys* **99**:113511–11356 (2006).
25 Bronze-Uhle ES, Batagin-Neto A, Xavier PHP, Fernandes NI, De Azevedo ER and Graeff CFO, *J Mol Struct* **1047**:102–108 (2013).
26 Piacenti-Silva M, Bronze-Uhle ES, Paulin JV and Graeff CFO, *J Mol Struct* **1056–1057**:135–140 (2014).
27 Wünsche J, Cicoira F, Graeff CFO and Santato C, *J Mater Chem B* **1**:3836–3842 (2013).
28 Wünsche J, Cardenas L, Rosei F, Cicoira F, Gauvin R, Graeff CFO *et al.*, *Adv Funct Mater* **23**:5591–5598 (2013).
29 Dezidério SN, Brunello CA, Da Silva MIN, Cotta MA and Graeff CFO, *J Non-Cryst Solids* **338–340**:634–638 (2004).
30 Kim YJ, Wu W, Chun S-E, Whitacre JF and Bettinger CJ, *Adv Mater* **26**:6572–6579 (2014).
31 Kim YJ, Wu W, Chun S-E, Whitacre JF and Bettinger CJ, *Proc Natl Acad Sci U S A* **110**:20912–20917 (2013).
32 Robertson J, *Adv Phys* **35**:317–374 (1986).
33 Capozzi V, Perna G, Gallone A, Biagi PF, Carmone P, Fratello A *et al.*, *J Mol Struct* **744–747**:717–721 (2005).
34 Perna G, Lasalvia M, Gallo C, Quartucci G and Capozzi V, *Open Surf Sci J* **5**:1–8 (2013).
35 Gonçalves PJ, Filho OB and Graeff CFO, *J Appl Phys* **99**:104701–104705 (2006).
36 Baraldi P, Capelletti R, Crippa PR and Romeo N, *J Electrochem Soc* **126**:1207–1212 (1979).
37 Jaber M and Lambert J-F, *J Phys Chem Lett* **1**:85–88 (2010).
38 Oliveira HP, Graeff CFO, Zanta CLPS, Galina AC and Gonçalves PJ, *J Mater Chem* **10**:371–375 (2000).
39 Simonovic BR and Wilczok T, *J Serb Chem Soc* **60**:981–986 (1995).
40 Swan GA and Waggott A, *J Chem Soc C* **10**:1409–1418 (1970).
41 Bloisi F, Pezzella A, Barra M, Alfè M, Chiarella F, Cassinese A *et al.*, *Appl Phys A* **105**:619–627 (2011).
42 Éhen Z, Novák C, Sztatisz J and Bene O, *J Therm Anal Calorim* **78**:427–440 (2004).
43 Shanmuganathan K, Cho JH, Iyer P, Baranowitz S and Ellison CJ, *Macromolecules* **44**:9499–9507 (2011).
44 Xu L and Weiss RA, *Polym Degrad Stab* **84**:295–304 (2004).
45 Roy BC, Gupta MD, Bhowmik L and Ray JK, *Synth Met* **100**:233–236 (1999).
46 Sajjan S, Kulkarni G, Yaligara V, Kyoung L and Karegoudar TB, *J Microbiol Biotechnol* **20**:1513–1520 (2010).
47 Gómez-Marín AM and Sánchez CI, *J Non-Cryst Solids* **356**:1576–1580 (2010).
48 Bridelli MG and Crippa PR, *J Phys Chem B* **114**:9381–9390 (2010).
49 Arzillo M, Mangiapia G, Pezzella A, Heenan RK, Radulescu A, Paduano L *et al.*, *Biomacromolecules* **13**:2379–2390 (2012).
50 Serpentini C-L, Gauchet C, Montauzon D, Comtat M, Ginestar J and Paillous N, *Electrochim Acta* **45**:1663–1668 (2000).
51 Gidanian S and Farmer PJ, *J Inorg Biochem* **89**:54–60 (2002).
52 Napolitano A, Pezzella A, d'Ischia M and Prota G, *Tetrahedron* **52**:8775–8780 (1996).